# Quantitative analysis of accuracy of an inertial/acoustic 6DOF tracking system.

Stuart J. Gilson[1], Andrew W. Fitzgibbon[2], Andrew Glennerster[1]

October 4, 2005

[1]: University Laboratory of Physiology,
Parks Road,
Oxford
OX1 3PT
United Kingdon
[2]: Department of Engineering Science,
Parks Road,
Oxford
OX1 3PJ
United Kingdon

**Pages (including figures and tables):** 26
**Figures:** 11
**Tables:** 1

**Corresponding author:** Stuart Gilson
University Laboratory of Physiology
Parks Road,
Oxford,
OX1 3PT
United Kingdom
Phone: +44 (0)1865 272460
Fax: +44 (0)1865 272469
Email: stuart.gilson@physiol.ox.ac.uk

## Abstract

An increasing number of neuroscience experiments are using virtual reality to provide a more immersive and less artificial experimental environment. This is particularly useful to navigation and three-dimensional scene perception experiments. Such experiments require accurate real-time tracking of the observer's head in order to render the virtual scene. Here we present data on the accuracy of a commonly used 6 degree of freedom tracker (Intersense IS900) when it is moved in ways typical of virtual reality applications. We compared the reported location of the tracker with its location computed by an optical tracking method. When the tracker was stationary, the root mean square error in spatial accuracy was 0.64mm. However, we found that errors increased over ten-fold (up to 17mm) when the tracker moved at speeds common in virtual reality applications. We demonstrate that the errors we report here are predominantly due to inaccuracies of the IS900 system rather than the optical tracking against which it was compared.

KEYWORDS: Virtual reality; Acoustic/inertial tracking; Psychophysics experiments; Active vision; Real-time measurements; Metric accuracy.

# 1 Introduction

Virtual reality is an increasingly common research tool in neuroscience (for example, see reviews by Tarr and Warren (2002), Bülthoff and van Veen (2001); Loomis et al. (1999) and a more skeptical view by Koenderink (1999)). Examples include work in sensory integration (Ernst et al., 2000) and sensori-motor control (Körding and Wolpert, 2004), spatial perception (Christou and Bülthoff, 1999; Tcheang et al., 2005; Sahm et al., 2005), navigation (Mallot and Gillner, 2000; Warren et al., 2001) and studies of social behaviour and psychiatric disorders (Slater et al., 2000; Freeman et al., 2005). There are clear advantages to using virtual reality given the flexibility and control it allows the experimenter. Equally, there are limitations to the technology that must be understood and accounted for when carrying out exeriments and interpreting the results.

In this paper we measure the spatial precision of one of the trackers used in a wide variety of experimental paradigms. Reporting the movement of the participant's head or limbs is the first and in some ways the most critical part of the chain of operations that link these movements to a change in the visual display. There are many different types of tracker. The criteria for choosing the most suitable for a given application include limitations on cost, precision and the volume of the tracked area required for experiments. The tracker we analyse here (an inertial/acoustic tracker supplied by Intersense) is currently cheaper than optical systems or mechanical arm trackers and covers a wider area. It is therefore an attractive option for many applications. However, the range and type of experiments that are appropriate depend on the accuracy and precision of the tracker. To design experiments that are commensurate with the quality of tracking, therefore, depends on reliable data on the performance characteristics of the tracking system that will be used, preferably under conditions similar to those that will be used in the experiment.

For example, in virtual reality experiments using small hand and finger movements, the position of the fingertip has been measured with very high accuracy using a PHANToM (SensAble Technologies). These devices not only provide information on the location of the fingertip (nominal accuracy of 0.02 mm) but also generate resisting force, allowing virtual haptic stimuli to be presented (Ernst et al., 2000; Körding and Wolpert, 2004). At a slightly larger scale, digitizing tablets have been used to track the position of limb (e.g GTCO Corporation, absolute accuracy about 0.1 mm (Baddeley et al., 2003)). Similar high accuracy tracking has been used to measure head position in virtual reality displays using a mechanical, multi-jointed arm but the range of head movement is restricted (e.g Panerai et al. (1999), nominal accuracy 0.6 mm within a range of about 0.5m in each directions). Magnetic trackers (Polhemus, Flock of Birds, Ascension) can be used to track the head but suffer from large spatial distortions outside a restricted spatial range.

Wider ranges of movement are possible with optical, inertial and acoustic tracking methods although again there is a trade off between precision and range of movement. Optical

methods fall into two categories, 'camera in' and camera out' methods (Ribo et al., 2001). Real-time 'camera in' systems (e.g. Vicon) use fixed calibrated cameras to compute the location of markers on the head or limb. The translation accuracy is high, e.g. less than 1mm offset and RMS, but the working volume is typically limited (some very large installations exist, but these are rare and extremely expensive). 'Camera out' systems, in which the camera is placed on the head while markers are placed in the scene (usually on the ceiling), have the advantage that they are very sensitive to head rotations. Accurate tracking of head rotation is particularly critical in augmented reality applications in which virtual objects are presented within real scenes (Azuma, 1997). One example is the Hi-Ball tracking system (Welch et al., 1999), which has been used in virtual reality experiments (Durgin et al., 2001) and can support movements over a considerable working volume (e.g. $40m^2$, spatial accuracy 0.2mm). Another is the recently available Intersense 'Vis-trak', which combines camera out tracking with an inertial sensor (Foxlin and Naimark, 2003) (3mm positional accuracy). An inertial sensor is also incorporated in the Intersense IS900 on which we report here (Foxlin et al., 1998). We have chosen to analyse the performance of the Intersense inertial/acoustic tracker (IS900) because it is one of the most frequently adopted trackers in experiments using virtual reality (Rolland et al., 2001; Sahm et al., 2005; Creem-Regehr et al., 2005; Foo et al., 2005; Slater et al., 2000).

For many applications, such as investigation of navigation (e.g Foo et al. (2005)), RMS errors in tracking of about 1 cm may well not affect the conclusions of an experiment. However, many experiments, for example investigating hand-eye coordination, require greater precision. A longer term goal should be the development of trackers that will allow freedom of movement and yet provide accurate tracking of hand and head movements and so increase the range and type of experiments that could be carried out. At present, a more limited goal is to characterise the spatial errors in tracking of systems to determine the range of experiments for which each is suitable.

The Intersense (Intersense Inc, Burlington, MA) IS900VET system is a hybrid acoustic and inertial system (Foxlin et al., 1998). Information from the inertial sensors and triaxial accelerometers in the tracking devices can be integrated twice to determine the tracker's position. These positional measurements are prone to drift and so are corrected by the ultrasonic acoustic system. Ultrasonic emitters are rigidly attached to the walls/ceiling of the tracked volume, and microphones on the tracking devices detect the emitted acoustic signal. The acoustic and inertial signals are combined, errors rejected, smoothed and the resulting position and orientation information transmitted to the host computer via a serial cable. The IS900 system works over a large volume (e.g. 12 m by 12 m in the VENlab, (Foo et al., 2005)), has a reported latency of $<$ 10ms, is relatively low cost compared to optical systems, and is sufficiently compact and light weight as to be unobtrusive.

The accuracy of the computed tracker position depends critically on careful calibration of the locations of the ultrasound emitters. Currently, this is done by surveying methods (using a theodolite). In the Discussion, we consider the theoretical improvements that could be gained

by using time-of-flight information to calculate the locations of the emitters. Mis-estimates of the emitter locations could account for variability in the reported tracker position.

The technical specifications for the IS900 give statistics for a static tracker—resolution of 1.5mm root mean square (RMS) error and an accuracy of 4mm RMS error (IS900 user manual)—but for an experimenter the error whilst the tracker is in motion is more relevant. Here we use on off-line optical tracking method to provide an accurate estimate of the true path followed by the tracker and compare this to the 3D locations reported by the IS900. We show that at typical walking speeds, errors are significantly above the static values. We discuss methods of calibration that might help improve the performance of this tracker and other types of tracker that could give higher accuracy while maintaining the freedom of movement that the IS900 allows.

## 2 Methods/Apparatus

We compared the IS900's reported positions with those derived from an independent tracking method. This second method did not need to be real-time, nor as robust (i.e. we could afford to re-conduct failed trials) as a real tracking system—but it did need to give reproducible positional estimates of the tracker to compare with the IS900's reported position of the same tracker. We used a purpose-built optical tracking system which comprised two IEEE-1394 cameras (A602fc, Basler AG, Germany) which streamed 640×480 pixel 8bpp mono digital images at 60Hz to the host computer (a desktop PC running GNU/Linux), which also received tracking information from the IS900 through a serial port. The host computer recorded the stream of video data and serial data to disk in real time, without skipping any frames. Having both video and coordinate data being received by the same computer allowed both to be synchronized—time stamps were recorded for the arrival of images and coordinates which subsequently allowed the two data sets to be temporally aligned (see figure 1).

The IS900 used Intersense's latest firmware (v4.14). Important settings relevant to tracking quality are – perceptual enhancement: 2 (default); prediction interval: 0ms (default); rotational sensitivity: 3 (default), ultrasonic emitter timeout: 20ms; ultrasonic emitter sensitivity: 1. The last two may vary between installations, but provide stable tracking in our laboratory. The tracked area was 3.50×3.54×3.13 m and used 51 ultrasonic emitters.

A bright LED was firmly attached to the tracker which was then moved by hand along a random path within a volume that was seen by both cameras. Images of the tracker and the tracker's position as reported by the IS900 were recorded during motion. Four conditions were studied, from a static tracker up to typical walking speeds (1m/s). Over a 20s period, images of the tracker were stored from the two cameras while at the same time position and orientation reports from the IS900 were recorded.

During recording, the operator moved the tracker in a random path within a volume visible

to both cameras (approximately $1m^3$). The LED is not at the tracked centre of the tracker (there is no marker denoting where this is on the physical tracker) and, hence, any rotation of the wand would cause a translation of the LED relative to this tracked centre. Since such translations would affect our tracking analysis, the tracker was held in a horizontal orientation as far as possible throughout the movement.

The location of the LED was extracted from the sequence of pairs of images yielding two arrays of 2D coordinates (one array from each camera). The images were thresholded to find bright regions, and a weighted centroid technique used to find the centre of the densest cluster of supra-threshold pixels. This centroid was measured to sub-pixel accuracy (see section 4.1) to give the position of the light source. The centroid coordinates were corrected for lens distortion.

Using standard photogrammetry techniques (Hartley and Zisserman, 2001), the path of the LED was reconstructed in three dimensions from these 2D coordinate arrays. This reconstructed path was in its own arbitrary coordinate system and had to be mapped into IS900 space before further analysis can be performed. A homography describes a one to one mapping of points from one projective coordinate frame to another—transforming each point in the reconstructed path by this homography allowed a direct point-by-point analysis of the reconstructed path and the IS900 recorded path to be performed. We found the homography that was maximally favourable to the IS900. Using the reconstructed data set as our 'ground truth' we were able to make spatial measurements of the errors in the IS900's tracking data.

[Figure 1 about here.]

## 3 Analysis

Figure 1 shows, for one tracker trajectory, part of the path recorded by the IS900 tracker (crosses) and, overlaid, the reconstructed path from the camera images (solid line). Taking the reconstructed optical path as the 'ground truth' (an assumption that we examine in section 4), we calculated the errors in the IS900 coordinates. Figure 2 summarizes the data for all trajectories, showing the errors as vectors, for the static, slow, medium and fast moving data sets. The error vectors have been rotated so that the $x$-component corresponds in each case to the direction of travel (as measured by the optical tracker). Figure 3 shows the magnitudes of the errors for the same conditions. The errors were slightly larger in the direction of travel (on average 1.3 times larger) but there was no systematic relationship between this ratio and the speed of the tracker.

Three recordings were made for each of the static, slow, medium and fast moving tracker conditions. The tracker's deviations from the optical path are shown in table I. The mean deviations at each sample point are 0.64, 2.86, 6.10 and 17.6mm respectively. The static error is well within the specification supplied by Intersense, but the non-static conditions, which

span the speeds used in 'typical' applications, have errors that increase with speed, and at the highest speed are significantly outside the quoted range.

[Table 1 about here.]

[Figure 2 about here.]

[Figure 3 about here.]

Figure 4 plots the magnitude of the IS900 spatial error over time for each of the four conditions. The errors for the static wand reveal several distinct regions or plateaus. These, we believe, result from the IS900 using a different set of ultrasonic emitters to determine the tracker's position at each plateau region and this—due to small calibration errors in the measurement of the location of these emitters—gives a different positional 'solution' (see figure 5). Figure 4 shows data for the moving conditions. The errors for the fast condition are significantly larger than for the slow condition (t = 54.09, d.f. = 2398, $p < 10^{-9}$).

[Figure 4 about here.]

[Figure 5 about here.]

Figure 6 shows how the speed of the tracker varied over the course of the moving conditions. Speeds were obtained by smoothing the optical and IS900 paths with a Gaussian kernel ($\sigma = 1$s) and taking first order differences (figure 6). There is evidence here of the IS900 failing to respond quickly to rapid changes in speed, which is characterised in the spatial domain as the IS900 trajectory over-running the true path of motion, as can be seen in figure 1. Figure 7 shows the RMS error in the three moving conditions plotted against speed. A linear fit to the slow, medium and fast data sets (figure 7) have slopes that are significantly different from zero.

[Figure 6 about here.]

[Figure 7 about here.]

Figure 8 shows acceleration profiles of a typical trajectory for the three moving conditions, where acceleration was calculated in the same way as speed, but now taking second order differences between smoothed samples. One might expect the largest errors between the IS900 and optical paths to occur during rapid changes of direction—equivalently regions of high acceleration. Figure 9 shows mean error against acceleration for the slow- and fast-moving cases. We again measured a linear fit to the 9 motion trajectories, but in this case found no consistent pattern (the range of slopes over all 9 moving trajectories was $-0.57s^2$ to $0.51s^2$). We believe, then, the difference in errors across conditions result from differences in speed not acceleration.

[Figure 8 about here.]

[Figure 9 about here.]

# 4 Sources of error

So far, we have used the reconstructed path for the optical tracking system as a measure of 'ground truth'. We consider here the extent to which this assumption is valid. The major known errors in the system arise from pixel errors in the optical stages and timing errors in receiving images from the camera and synchronizing these with the IS900 samples.

## 4.1 Pixel errors

Pixel errors arose from the extraction of the light source in the video images. Image noise and numerical errors in this thresholding process could have led to inaccuracies in this process. However, the standard deviation of the centroid extracted from images of a static light source was less than a tenth of a pixel. To see how image noise affects our analysis of IS900 data, we deliberately added Gaussian distributed random noise to the extracted image coordinates, and repeated the whole extraction process to determine how RMS error increases with increasing standard deviation of noise (figure 10). For standard deviations below 0.5 pixels, the RMS error barely changes and, hence, pixel errors are unlikely to have contributed significantly to overall RMS error.

[Figure 10 about here.]

## 4.2 Temporal misalignment

The synchronization of the images captured by the two cameras and the IS900 coordinates at the moment of capture are important. Increasing delays between the capture of the two images will result in reconstruction errors (notably in the depth of the reconstructed point), and delays between image capture and IS900 coordinate capture will make mapping one path onto the other difficult.

Although time stamps were recorded for the arrival of images and IS900 coordinates at the host computer and were used in the subsequent fitting process, it is still possible that the image pair that arrived at time $t$ fits better with the IS900 coordinate that arrived at time $t+\varepsilon$ than the coordinate that also arrived at time $t$. Therefore, we repeated our transformation of the optical path onto IS900 path using different values of $\varepsilon$ (see figure 11). There was a negligible reduction in RMS error between $\varepsilon = 0$ms and the best fit ($\varepsilon = 21$ms).

[Figure 11 about here.]

### 4.3 Measuring IS900 error by plane fitting

We wanted to asses IS900 error without relying on our optical system, in order to verify that the optical system introduces negligible error. We did this by mounting the tracker on a turntable to restrict its motion to a plane, and measuring the perpendicular error to the best-fitting plane through the IS900 data. The speed of motion was comparable to the previous medium speed condition. We found an RMS error of 2.7mm perpendicular to the plane. This is similar in magnitude to the error perpendicular to the direction of travel in the freely moving tracker condition (medium speed, 3.1mm), suggesting that the errors in both cases arise predominantly from the IS900 tracker. The planar movement test alone is not an adequate test of the tracker performance as it cannot identify the component of error in the direction of travel nor can it identify situations where the IS900 has 'over run' the true trajectory as we have illustrated happening at points of rapid change in direction.

## 5 Discussion

We have analysed one of the more commonly used tracking systems used in virtual reality experiments and report the precision of this system (Intersense VET) over a range of tracker speeds. Performance deteriorates with increasing tracker speed so that, at typical walking speeds, errors are approximately 4 times those quoted for a static tracker. As we have argued in the Introduction, an accurate assessment of the reliability of the tracker position estimate is critical when designing experiments. It is necessary in order to judge the extent to which the visual stimulus might differ from the correct one. Also, if the tracker output is being used to report the subject's movements (for example in intercepting a ball), the device's precision must be known. Of the types of experiments carried out to date using the IS900, many are unlikely to be seriously affected by tracking errors of the magnitude reported here, including experiments on navigation (e.g. Foo et al., 2005) or social interactions (e.g. Slater et al., 2000). By contrast, detailed studies of object manipulation or hand-eye coordination would be likely to suffer, both in generation of a reliable stimulus and in records of the head and hand position.

We have assumed that it is valid to treat the position estimate derived from the optical tracking system as 'ground truth'. Specifically, section 4 lists the potential sources of error in the optical tracking system and the ways in which we have ensured that these errors were kept to a minimum. We have shown that some errors would not have a significant effect on the computed optical tracking path even if they had been significantly larger (figure 10).

We have suggested that the predominant source of errors in the IS900 system is likely to be variations in calibration between different sub-sets of emitters. We have direct evidence for this when the tracker is stationary: in this case errors correlate with changes in the subset of emitters used (figure 5). The increase in errors with increasing tracker speed we found is

consistent with the hypothesis that moving between different subsets of chirpers is the main cause of the errors.

There are a number of ways in which this problem might be tackled. In our opinion, transition between detector subsets can be smooth for a correctly calibrated system. The reason that abrupt transitions remain a perennial problem is that this calibration is extremely difficult in practice. We have made progress towards ameliorating this problem by adapting techniques from photogrammetric bundle adjustment (Duff and Muller, 2003), but these techniques are not yet proved in real-world application. When inertial/acoustic systems can be calibrated accurately they should provide substantially improved tracking in addition to the advantages of cost and range that they have at the present.

In principle, the problem of moving between subsets of sensors applies equally to optical systems,but these are routinely calibrated using bundle-adjustment techniques, and do not exhibit such mis-measurement errors. It remains to be seen whether optical tracking systems will provide an accurate, cheap and robust alternative to inertial/acoustic tracking systems.

## 6 Acknowledgements

Supported by the Wellcome Trust and the Royal Society.

## References


Azuma, R. T. (1997). A survey of augmented reality. *Presence: Teleoperators and Virtual Environments*, 6(4):355–385.

Baddeley, R. J., Ingram, H. A., and Miall, R. C. (2003). System identification applied to a visuomotor task: near-optimal human performance in a noisy changing task. *Journal of Neuroscience*, 23(7):3066–3075.

Bülthoff, H. H. and van Veen, H. A. H. C. (2001). Vision and action in virtual environments: Modern psychophysics in spatial cognition research. In Jenkin, M. and Harris, L., editors, *Vision and Attention*, pages 233–252. Springer-Verlag, New York, USA.

Christou, C. G. and Bülthoff, H. H. (1999). View dependence in scene recognition after active learning. *Memory and Cognition*, 27(6):996–1007.

Creem-Regehr, S. H., Willemsen, P., Gooch, A. A., and Thompson, W. B. (2005). The influence of restricted viewing conditions on egocentric distance perception: Implications for real and virtual environments. *Perception*, 34(2):191–204.

Duff, P. and Muller, H. (2003). Autocalibration algorithm for ultrasonic location systems. In *Proceedings of the Seventh IEEE International Symposium on Wearable Computers*, pages 62–68. IEEE Computer Society.

Durgin, F. H., Gigone, K., and Scott, R. (2001). Perception of visual speed while moving. *Journal of Experimental Psychology: Human Perception and Performance*, 31(2):339–353.

Ernst, M. O., Banks, M. S., and Bülthoff, H. H. (2000). Touch can change visual slant perception. *Nature Neuroscience*, 3(1):69–73.

Foo, P., Warren, W. H., Duchon, A., and Tarr, M. J. (2005). Do humans integrate routes into a cognitive map? Map- versus landmark-based navigation of novel shortcuts. *Journal of Experimental Psychology: Learning, Memory, and Cognition*, 31(2):195–215.

Foxlin, E., Harrington, M., and Pfeifer, G. (1998). Constellation: a wide-range wireless motion-tracking system for augmented reality and virtual set applications. In *Proceedings of the 25th annual conference on Computer graphics and interactive techniques*, pages 371–378. ACM Press.

Foxlin, E. and Naimark, L. (2003). VIS-Tracker: A wearable vision-interial self-tracker. In *IEEE VR2003, March 22–26, Los Angeles, USA*.

Freeman, D., Garety, P. A., Bebbington, P., Slater, M., Kuipers, E., Fowler, D., Green, C., Jordan, J., Ray, K., and Dunn, G. (2005). The psychology of persecutory ideation II: A virtual reality experimental study. *Journal of Nervous & Mental Disease*, 193(5):309–315.

Hartley, R. and Zisserman, A. (2001). *Multiple view geometry in computer vision*. Cambridge University Press, UK.

Koenderink, J. J. (1999). Virtual psychophysics. *Perception*, 28:669–674.

Körding, K. P. and Wolpert, D. M. (2004). Bayesian integration in sensorimotor learning. *Nature*, 427:244–247.

Loomis, J. M., Blascovich, J. J., and Beall, A. C. (1999). Immersive virtual environment technology as a basic research tool in psychology. *Behavior Research Methods, Instruments and Computers*, 31:557–564.

Mallot, H. A. and Gillner, S. (2000). Route navigating without place recognition: What is recognised in recognition-triggered responses? *Perception*, 29(1):43–55.

Panerai, F., Hanneton, S., Droulez, J., and Cornilleau-Pérès, V. (1999). A 6-dof device to measure head movements in active vision experiments: geometric modelling and metric accuracy. *Journal of Neuroscience Methods*, 90:97–106.

Ribo, M., Pinz, A., and Fuhrmann, A. (2001). A new optical tracking system for virtual and augmented reality applications. In *Proceedings of 18th IEEE Instrumentation and Measurement Technology Conference, Budapest, Hungry*, volume 3, pages 1932–1936.

Rolland, J. P., Davis, L. D., and Baillot, Y. (2001). A survey of tracking technologies for virtual environments. In Barfield, W. and Caudell, T., editors, *Fundementals of Wearable Computers and Augmented Reality*. Lawrence Erlbaum Assoc, Mahwah, NJ.

Sahm, C. S., Creem-Regehr, S. H., Thompson, W. B., and Willemsen, P. (2005). Throwing versus walking as indicators of distance perception in similar real and virtual environments. *ACM Transactions on Applied Perception*, 2(1):35–45.

Slater, M., Sadagic, A., Usoh, M., and Shroeder, R. (2000). Small-group behaviour in a virtual and real environment: A comparative study. *Presence: Teleoperators and Virtual Environments*, 9(1):37–51.

Tarr, M. J. and Warren, W. H. (2002). Virtual reality in behavioral neuroscience and beyond. *Nature Neuroscience*, 5:Supplement 1089–1092.

Tcheang, L., Gilson, S. J., and Glennerster, A. (2005). Systematic distortions of perceptual stability investigated using immersive virtual reality. *Vision Research*, 45:2177–2189.

Triggs, W., McLauchlan, P., Hartley, R., and Fitzgibbon, A. (2000). Bundle adjustment: A modern synthesis. In Triggs, W., Zisserman, A., and Szeliski, R., editors, *Vision Algorithms: Theory and Practice*, LNCS. Springer Verlag.

Warren, W. H., Kay, B. A., Zosh, W. D., Duchon, A. P., and Sahuc, S. (2001). Optic flow is used to control human walking. *Nature Neuroscience*, 4(2):213–216.

Welch, G., Bishop, G., Vicci, L., Brumback, S., Keller, K., and Colucci, D. (1999). The HiBall tracker: High-performance wide-area tracking for virtual and augmented environments. In *Symposium on Virtual Reality Software and Technology*, pages 1–10.

# List of Figures

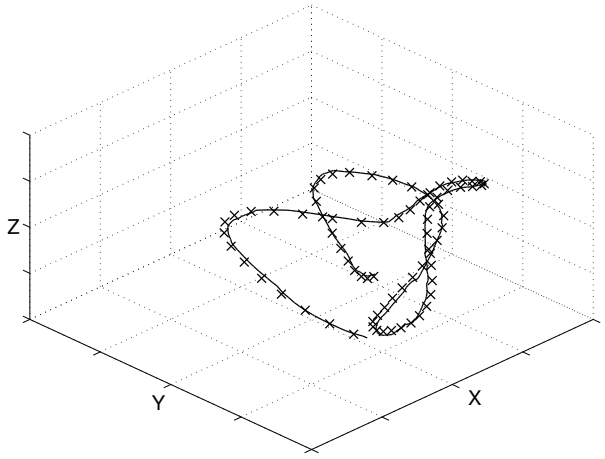


Figure 1: Path reconstructed from pairs of 2D images (solid line) with IS900 path (crosses) overlaid. Only a short segment of the path is shown (with only every fifth IS900 coordinate shown for clarity) but deviations between the two paths can still be seen, especially during rapid changes of direction.

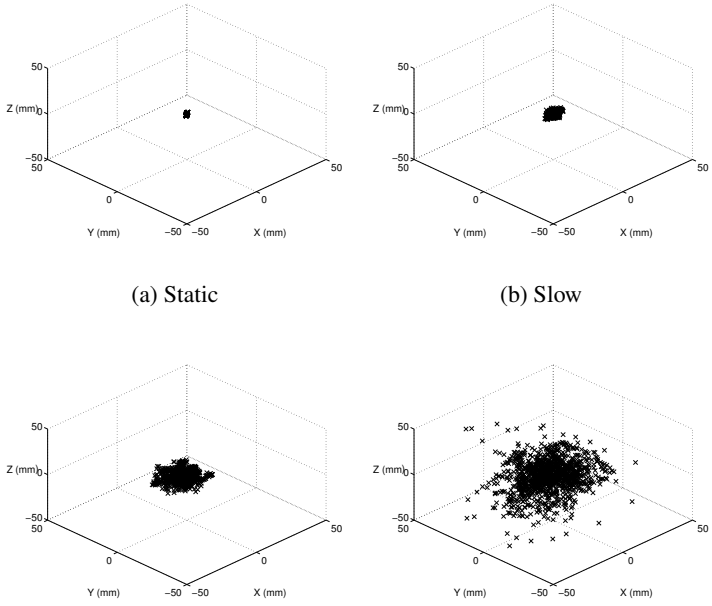


(a) Static (b) Slow

(c) Medium (d) Fast

Figure 2: Error vectors between IS900 and optical paths for static, slow, medium and fast moving cases. Error vectors have been rotated to aligned so that the $x$-axis corresponds to the tracker's direction of travel. RMS errors along and perpendicular to the direction of travel were 2.0 and 1.4mm for the slow condition; 4.3 and 3.1mm for the medium condition; and 10.9 and 9.9mm for the fast condition.

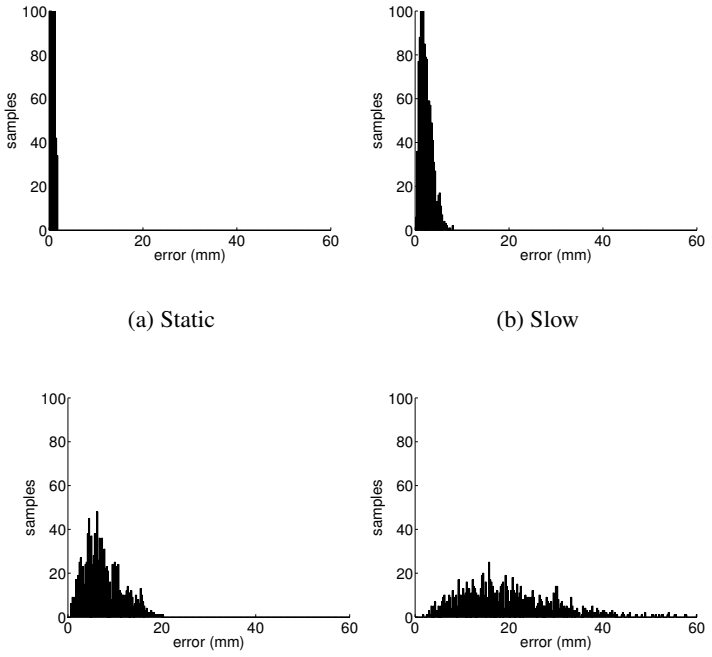


(a) Static (b) Slow

(c) Medium (d) Fast

Figure 3: Histograms of spatial error magnitudes for static, slow, medium and fast moving cases. To aid comparison, the axis for figures (a) and (b) have been clipped at 100 samples.

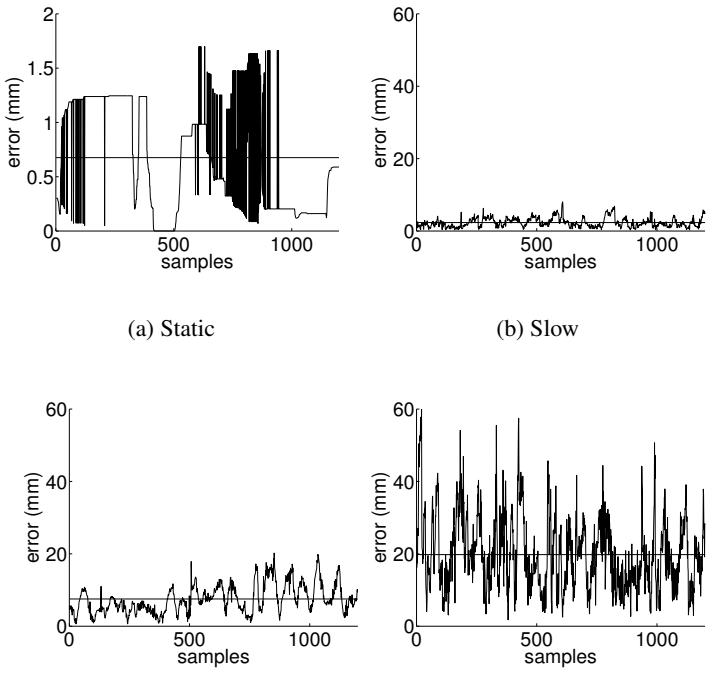


(a) Static

(b) Slow

(c) Medium

(d) Fast

Figure 4: Spatial errors between IS900 and optical paths for each sample point. The plot for the static condition (a) has a different axis scale to reveal the sudden spatial 'jumps' the IS900 makes even when the tracker is stationary.

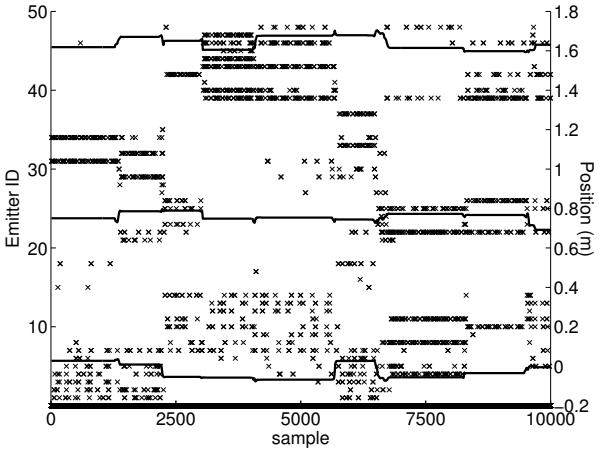


Figure 5: The X, Y and Z components of position reported by a static IS900 tracker (middle, top and bottom solid black lines respectively), overlaid onto a plot of the ultrasonic emitters active during each sample (crosses). Changes in reported tracker position coincide with changes in the subset of ultrasonic emitters used by the IS900.

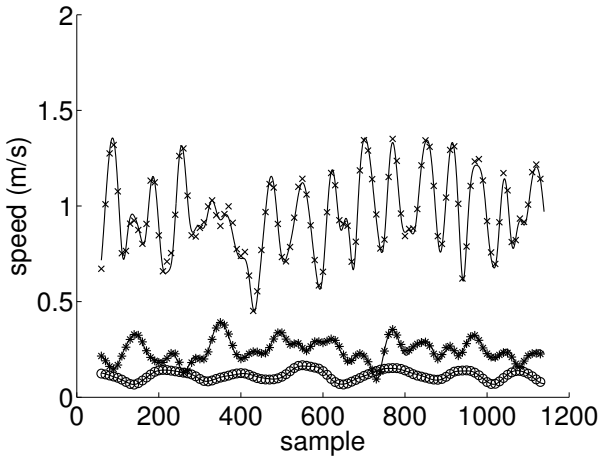


Figure 6: Speed profiles for the slow (circles), medium (stars) and fast (crosses) conditions showing IS900 versus optical path (solid line). Only 1 in 15 points shown here for clarity. Deviations between IS900 and optical paths are apparent at large changes in speed.

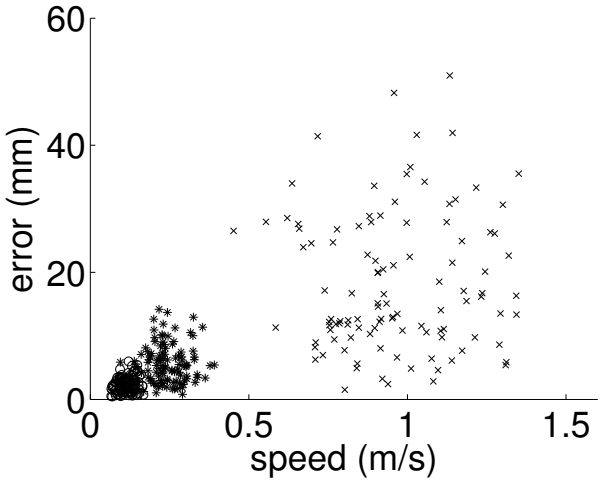


Figure 7: RMS error plotted against IS900 tracker speed for the slow (circles), medium (stars) and fast (crosses) conditions. Only 1 in 15 points shown here for clarity. The slopes of linear fits through the data have slopes for the slow condition were: $0.0039 \pm 0.00057$ mm/m/s ($t = 6.91$, $p < 10^{-9}$); medium: $0.0128 \pm 0.0011$ mm/m/s ($t = 12.15$, $p < 10^{-9}$); fast: $0.0037 \pm 0.00066$ mm/m/s ($t = 5.59$, $p < 10^{-9}$).

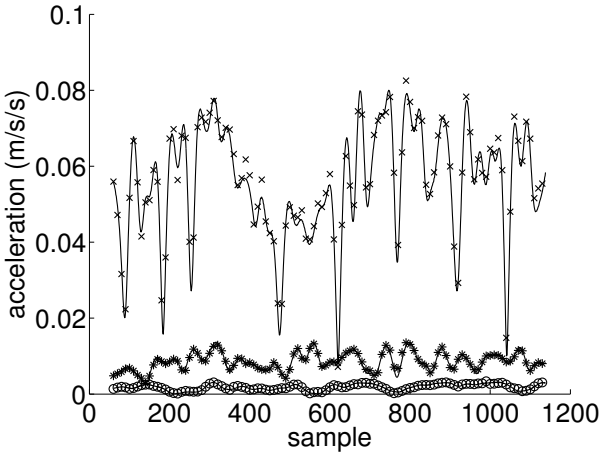


Figure 8: Acceleration profiles for the slow (circles), medium (stars) and fast (crosses) conditions for the IS900 positions versus optical path (solid line). Only 1 in 15 points shown here for clarity.

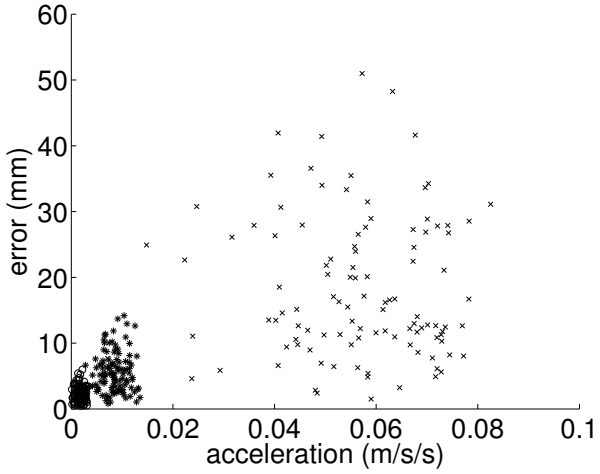


Figure 9: RMS error plotted against IS900 acceleration for the slow (circles), medium (stars) and fast (crosses) conditions. Only 1 in 15 points shown here for clarity.

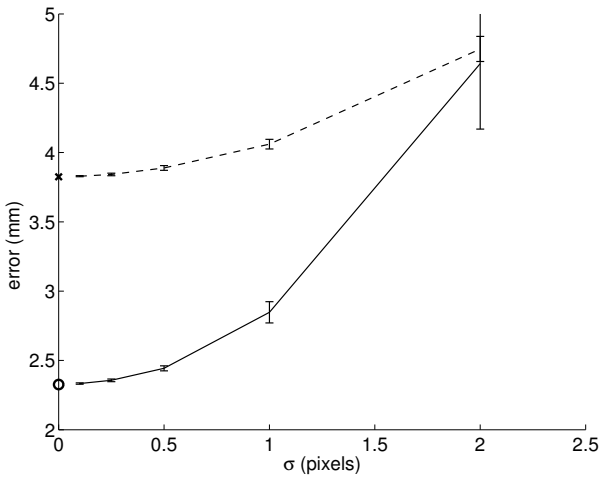


Figure 10: RMS error increasing with increasing standard deviation of the Gaussian distributed noise (mean over 200 trials). Error bars show standard deviation. Solid line is for a typical 'slow' IS900 tracker path, while the dashed line is for a typical 'medium' path. The circle and cross symbols denote the RMS error for the slow and medium paths without added image noise.

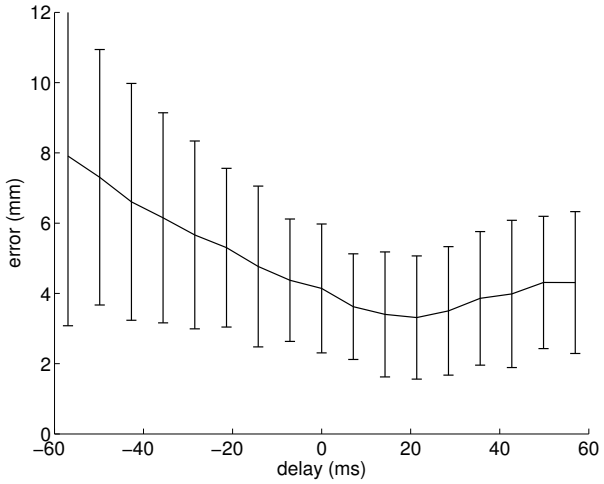


Figure 11: RMS error changing with different temporal alignments of image and IS900 data sets, for a typical slow IS900 path. IS900 coordinates arrive at intervals of approximately 7ms. The best fit between the two data sets is when the image coordinates are fitted to IS900 coordinates 21ms later than the ideal time stamp match. Even so, the difference between no delay and this optimum delay is less than 0.5mm RMS error at each sample point.

## List of Tables

| Recording | Static | Slow | Medium | Fast |
|---|---|---|---|---|
| 1 | 0.846±0.51mm | 2.66±1.3mm | 4.59mm±2.5mm | 20.1mm±10mm |
| 2 | 0.716±0.25mm | 3.11±1.5mm | 8.50mm±3.2mm | 15.0mm±6mm |
| 3 | 0.357±0.28mm | 2.81±1.4mm | 5.23mm±3.2mm | 17.4mm±8mm |

Table I: Mean deviation at each sample point of the IS900 tracker from the optical path for static, slow- and fast-moving conditions.